Ir- and Ru-doped layered double hydroxides as affordable heterogeneous catalysts for electrochemical water oxidation

Fagiolari, Lucia ; Zaccaria, Francesco ; Costantino, Ferdinando ; Vivani, Riccardo ; Mavrokefalos, Christos K ; Patzke, Greta R ; Macchioni, Alceo

Abstract: Three M-doped LDHs (M = noble metal active site, LDH = layered double hydroxides; Ir-1, Ir-ZnAl; Ru, Ru-ZnAl; Ir-2, Ir-MgAl), containing small amounts of M (ca. 2 mol% and even <1 mol% for Ru and Ir, respectively), were prepared by following simple and established synthetic procedures. Their characterization indicates that M atoms are effectively incorporated into the brucite-like layers of LDH, without phase segregation. The resulting materials catalyse electrochemical water oxidation (WO), when immobilized in carbon paste electrodes, with performances that exceed those of the benchmark system IrO2, as probed by linear sweep voltammetry (LSV). Some of these catalysts undergo continuous activation upon chronoamperometric and chronopotentiometric treatments over several hours. The crystalline structure of all of them is preserved during electrocatalytic experiments, and no significant leaching of noble metal in solution is detected. The results herein reported highlight the remarkable potential of these doped M-LDHs and confirm that dispersing Ir and Ru centers in layered and cheap inorganic materials results in easily accessible metal centers, providing highly active catalysts, while minimizing the utilization of noble metals.

DOI: https://doi.org/10.1039/c9dt04306c

Ir- and Ru-doped layered double hydroxides as affordable heterogeneous catalysts for electrochemical water oxidation

Lucia Fagiolari,[a,b] Francesco Zaccaria,[a] Ferdinando Costantino,[a] Riccardo Vivani,[c] Christos Mavrokefalos,[d] Greta R. Patzke[d,*] and Alceo Macchioni[a,*]

Three M-doped LDHs (M = noble metal active site, LDH = layered double hydroxides; **1**, Ir-ZnAl; **2**, Ru-ZnAl; **3**, Ir-MgAl), containing small amounts of M (ca. 2 mol % and even <1 mol % for Ru and Ir, respectively), were prepared by following simple and established synthetic procedures. Their characterization indicate that M atoms are effectively incorporated into the brucite-like layers of LDH, without phase segregation. The resulting materials catalyse electrochemical water oxidation (WO), when immobilized in carbon paste electrodes, with performances that exceed those of the benchmark system IrO_2, as probed by linear sweep voltammetry (LSV). Some of these catalysts undergo continuous activation upon chronoamperometric and chronopotentiometric treatments over several hours. The crystalline structure of all of them is preserved during electrocatalytic experiments, and no significant leaching of noble metal in solution is detected. The results herein reported highlight the remarkable potentialities of these doped M-LDHs and confirm that dispersing Ir and Ru centers in layered and cheap inorganic materials results in easily accessible metal centers, providing highly active catalysts, while minimizing the utilization of noble metals.

Introduction

Whatever strategy for the production of renewable solar fuels could be imagined, it necessarily requires a source of electrons and protons coming from a cheap and abundant raw material, possibly water. This is the reason why water oxidation (WO) has become one of the most studied reactions, over the last decades, especially as far as the development of a catalyst (C) for its acceleration is concerned.[1–6] Significant, but still technologically unsatisfactory,[7] results have been achieved by using homogeneous,[8–17] heterogenized,[18–24,25] and heterogeneous[26–33] WOCs. The best performances are usually obtained by using noble-metal (e.g. M = Ru and Ir)[34–37] based WOCs, both in terms of TOF and, especially, TON. Consequently, two main strategies have been pursued by the scientific community, which are the development of earth-abundant WOCs with improved performances[38-40] and the minimization of noble atom content in noble-metal based WOCs, according to the noble-metal atom economy concept.[34,41] Minimization of the amount of noble-metal in WOCs, with respect to bulk materials, might be achieved by i) using molecular catalysts, which usually have higher activity and higher percentage of active centers, ii) anchoring a molecular catalyst onto a suitable selected support, and iii) by diluting the active centers in a proper material, having features that maximize M-accessibility and performance. Strategies i) and ii) have their main drawback in the stability of the molecular catalyst under the harsh conditions of WO.[42,43] In addition, leaching of the active sites might be a problem for strategy ii). The main difficulty for pursuing strategy iii) lies in finding the right materials.

Recently, we showed that layered double hydroxides (LDHs),[44,45] based on earth-abundant elements, are suitable starting materials to host tiny amounts of noble metals, providing efficient WOCs.[46] Their brucite-like structure is characterized by positively charged hydroxide sheets, which are separated by interlayer regions where the counterions are intercalated.[47] This architecture is related to that of heterogeneous WOCs based on layered semiconductors, in which the high charge density of the 2D interlayer spaces is easily accessible for electrons and water molecules, facilitating charge transfer.[48,49] With respect to the latter systems, based - for instance- on metal oxides[28,50] and perovskites,[51] LDHs offer the advantage of being very cheap and easily accessible compounds, which can be effectively hybridized and functionalized with a variety of materials for a broad range of applications,[52–58] including those based on the oxygen evolution reaction (OER).[49,59-61]

Thus, in the aforementioned seminal paper,[46] a ZnAl LDH was functionalized with highly dispersed Ir(III) atoms (<3 mol % with respect to the total metal content), which were effectively incorporated in the brucite-like layers without phase segregation. The resulting material $[Zn_{0.667}Al_{0.306}Ir_{0.027}(OH)_2]Cl_{0.333}{\cdot}0.6H_2O$ showed high catalytic activity towards WO driven by $NaIO_4$ as sacrificial oxidant (SO) with TOF up to 113 min^{-1}, and a notably high TON > 11900. The high

[a] Department of Chemistry, Biology and Biotechnology, Università di Perugia and CIRCC- Via Elce di Sotto 8, I-06123 Perugia, Italy.
[b] Department of Applied Science and Technology, Politecnico di Torino - Corso Duca degli Abruzzi 24, I-10129 Torino, Italy.
[c] Department of Pharmaceutical Sciences, Università di Perugia - Via del Liceo 1, I-06123 Perugia, Italy.
[d] Department of Chemistry, University of Zurich - Winterthurerstrasse 190, CH-8057 Zurich, Switzerland.
† E-mail: alceo.macchioni@unipg.it, greta.patzke@chem.uzh.ch
Electronic Supplementary Information (ESI) available: Additional details on synthesis, characterization and catalytic tests. See DOI: 10.1039/x0xx00000x

efficiency of these systems compares well with that of molecular organometallic WOCs[62-64] and, at the same time, is combined with very high recyclability and no appreciable leaching of the Ir centers in the liquid phase, as assessed by ICP-OES analysis on both the reaction medium and the solid after catalytic tests. Therefore, Ir-doped LDHs are very robust, high-performing and relatively cheap heterogeneous WOCs.

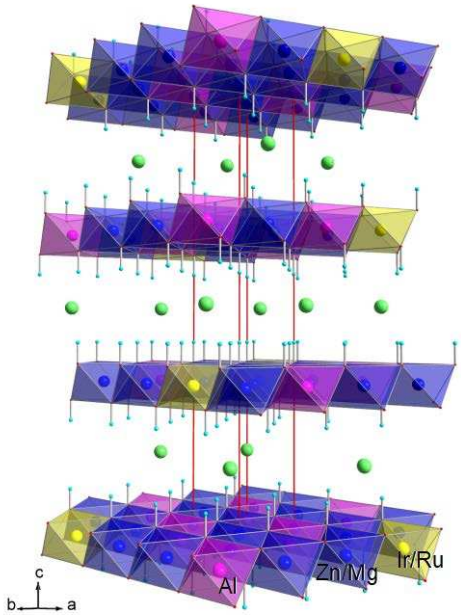

Fig. 1 Polyhedral representation of the crystal structure of a layered double hydroxide doped with Ir or Ru. Metal cations are randomly distributed in the brucitic sheets. Unit cell axes are in red colour.

Herein, the potential application of noble-metal functionalized LDHs (M-LDH; M = noble metal) in electrochemical rather than SO-driven WO is explored, providing more comparable results with other heterogeneous systems reported in the literature. In particular, three systems with different compositions have been considered, differing with respect to the nature of the active metal (Ir *vs.* Ru) and the bulk inorganic cations (Zn^{2+}, Al^{3+} *vs*. Mg^{2+}, Al^{3+}, Fig. 1). Commercial iridium oxide (**IrO_2**), a known heterogeneous WOC,[65] was used as internal benchmark, and a non-functionalized ZnAl LDH was included in the screening as blank test (**B**). The structure of the synthesized LDHs was characterized before and after the catalytic experiments. Furthermore, chronoamperometry and chronopotentiometry studies were carried out to evaluate the durability of these systems.

Results and Discussion

Synthesis and characterization of M-LDHs

M-LDHs were prepared by refluxing a water solution of the proper chloride salts in the presence of urea as crystallizing agent (see ESI for details).[46,66,67] The products precipitated as white powders, which were isolated by filtration, washed with CO_2-free water to prevent carbonate contamination, and finally dried at 60°C. The metal composition of the three M-LDHs and of the noble-metal free species was determined by ICP-OES analysis, resulting in the following molecular formulae:

B: $[Zn_{0.61}Al_{0.39}(OH)_2](Cl)_{0.39}\cdot 0.6H_2O$;
Ir-1: $[Zn_{0.647}Al_{0.349}Ir_{0.004}(OH)_2](Cl)_{0.353}\cdot 0.6H_2O$;
Ru: $[Zn_{0.65}Al_{0.33}Ru_{0.02}(OH)_2](Cl)_{0.35}\cdot 0.6H_2O$;
Ir-2: $[Mg_{0.647}Al_{0.349}Ir_{0.004}(OH)_2](Cl)_{0.353}\cdot 0.6H_2O$.

It is worth emphasizing that the noble-metal content with respect to the total cations is around 2 mol % for **Ru** and well below 1 mol % for **Ir-1** and **Ir-2**, that is, even lower than that of the previously reported Ir-LDH (ca. 3 mol %).[46]

Fig. 2 shows the powder X-ray diffraction (PXRD) patterns of the four synthesized LDHs. All of them closely correspond to literature data for ZnAl-Cl LDH.[68] Rietveld refinement of the four dataset,[69] allowed to detect the presence of the sole brucitic LDH phase for all the samples. Fig. S1-S4 in the ESI show the final difference plots relating to the above procedure, while Table S1 reports the refined unit cell parameters and the statistic agreement factors of the whole refinements. The refined unit cell parameters for **Ir-1** and **Ir-2** were found to not differ significantly from those of the pristine LDH phases, while for **Ru** the *a* parameter, which is related to the metal-to-metal spacing within the brucitic sheet, was found 0.3% larger than that of pure ZnAl-Cl phase.[68] Taking into account that Ir(III) and Ru(III) have ionic radii slightly higher than that of Al(III) in octahedral coordination (0.68 and 0.62 *vs*. 0.53 Å, respectively),[70] and also considering their contents in the three samples, these results substantially confirm, at least for Ru, their effective incorporation in the brucitic structure, in line with the results reported by Vaccari and co-workers.[71]

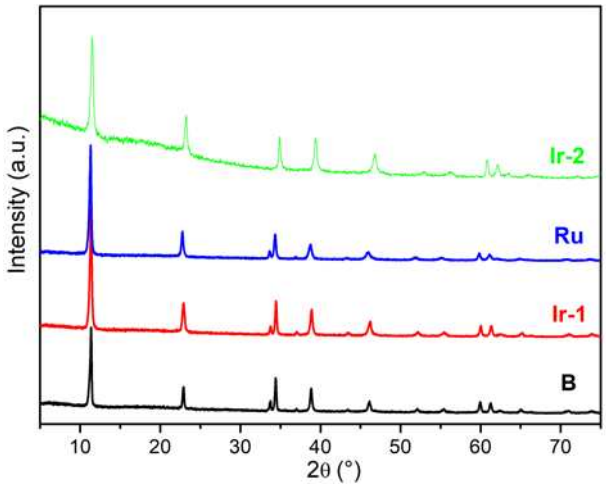

Fig. 2 PXRD patterns of undoped reference LDH (**B**) and of the three doped M-LDH (**Ir-1**, **Ru** and **Ir-2**).

FT-IR characterization was carried out as well (Fig. S5). All the typical peaks of a pure LDH phase are observed also for the three doped M-LDHs, such as water bending at 1615 cm^{-1}, O-H stretching at 3400 cm^{-1} and O-metal bending at 560 cm^{-1}

(Table S2). Carbonate stretching modes at about 1414 cm^{-1} are detected, indicating a small contamination with CO_3^{2-} anions, which is however not detected in PXRD analyses. It is known that variations of the FT-IR peak positions can be diagnostic of metal incorporation in LDHs.[72-73] Here, the small but appreciable shift of the O-metal stretching band towards higher wave numbers, proceeding from **B** to **Ir-1** and **Ru,** is consistent with the incorporation of tiny amounts of heavy atoms like Ir and Ru, which results in higher energies required for this stretching mode. SEM images (Fig. S6) show aggregates of homogenously shaped particles with micrometric dimensions for each sample, while a sand-rose morphology is more pronounced for **Ir-2**, as usually found in MgAl LDH samples.[66]

M-LDHs activity in electrochemical WO

The three synthesized M-LDHs were tested as heterogeneous catalysts for electrochemical WO under the same experimental conditions, using a standard three-electrode cell (see Experimental Section for details). M-LDHs were mixed with carbon paste in a 60:40 w/w ratio and pressed in a carbon paste working electrode. LDHs are known to efficiently couple with typical electrode materials, like the carbon paste used here, facilitating electron conductivity.[54,56] A platinum wire and Ag/AgCl (KCl 3M)[74] were used as counter and reference electrodes, respectively. All experiments were carried out in a 1 M KOH electrolyte solution, under typical conditions used with LDH-based catalysts,[56,75] probing OER by linear sweep voltammetry (LSV). High-performing WOCs are expected to generate high current densities (J) at low applied overpotentials (η). Fig. 3 shows the current density profiles measured at the working electrode for the systems of interest. Blank experiments show that the LDH without noble metal (**B**), as well as the mere carbon paste, generate at most negligible current densities (even up to η = 700 mV), indicating that these raw materials are catalytically inert under the reaction conditions explored here. Conversely, all three doped M-LDHs are capable to effectively catalyse WO with current densities that are comparable (**Ir-2**) or even higher (**Ir-1** and **Ru**) than that of the benchmark system **IrO_2**. In particular, current density at 280 mV (J_{280}) is 2.4 mA/cm^2 for **Ir-1**, 11.3 mA/cm^2 for **Ru**, 1.5 mA/cm^2 for **Ir-2** and 1.3 mA/cm^2 for **IrO_2** (Table 1). Furthermore, **Ir-1** and, especially, **Ru** outperform **IrO_2** also in terms of overpotential at 10 mA/cm^2 current density (η_{10}),[76] resulting in the following order: **Ru** (245 mV) < **Ir-1** (345 mV) < **IrO_2** (384 mV) < **Ir-2** (458 mV; Table 1). The performance of the benchmark system, in terms of η and J, is comparable to that of similar iridium oxide-based WOCs reported in the literature.[77,78] The formation of molecular oxygen was probed by gas chromatography (GC) for selected cases (see ESI); the ability of analogous M-LDHs to generate oxygen has been also previously proved by monitoring WO driven by $NaIO_4$ with the Clark electrode.[46]

These trends are confirmed by those derived from the Tafel slopes, which were evaluated by plotting the overpotential as a function of the logarithm of the current density in the linear region 0 < log(J) < 1 (Fig. S9). The good performances of **Ir-1** and **Ru** are reflected by their appreciably lower Tafel slopes (92 and 85 mV/dec, respectively; Table 1) with respect to **IrO_2** (102.7 mV/dec) and **Ir-2** (167 mV/dec). The very high Tafel slope of 178 mV/dec found for **B**, as well as its low performance with respect to J_{280} and η_{10} (Table 1), are indicative of the negligible catalytic properties of this undoped LDH, as previously mentioned.

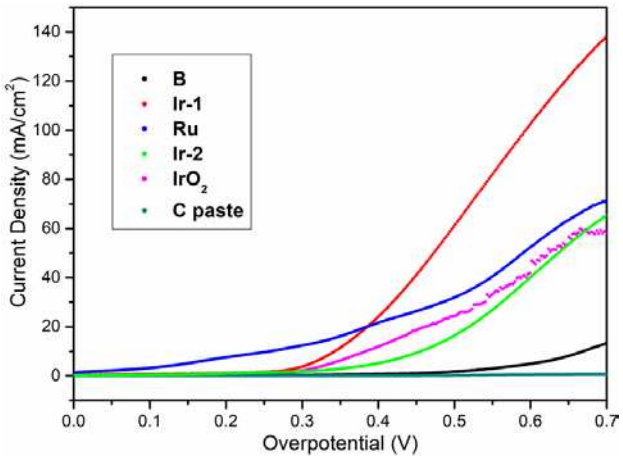

Fig. 3 Representative current density *vs.* overpotential profiles obtained in electrocatalytic experiments by LSV (25°C, 1 M KOH, scan rate 1 mV/s).

Table 1 Electrocatalytic performance from electrocatalytic tests of all compounds. [a]

Entry	Catalyst	J_{280} (mA/cm^2)	η_{10} (mV)	Tafel slope (mV/dec)[b]	TOF (10^{-3} s^{-1})[c]
1	**B**	0.21 ± 0.02	670 ± 2	178 ± 2	-
2	**Ir-1**	2.4 ± 0.3	345 ± 2	92.0 ± 0.3	1.46 ± 0.09
3	**Ru**	11.3 ± 0.6	245 ± 7	85 ± 4	1.89 ± 0.04
4	**Ir-2**	1.5 ± 0.3	458 ± 2	167 ± 18	0.68 ± 0.06
5	**IrO_2**	1.3 ± 0.6	384 ± 2	102.7 ± 0.2	0.0037 ± 0.0008
6	**C paste**	0.002	-	-	-

[a] 25°C, 1 M KOH, 1mV/s scan rate; [b] determined in the linear region 0 < log(J) < 1; [c] determined by the electrochemical equation TOF = $J \times A/(4F \times m)$, where A is the geometrical area of the electrode, F is the Faraday constant, m is the number of moles of active noble metal centers.[49] J_{280} = current density at 280 mV; η_{10} = overpotential at 10 mA/cm^2; C paste = carbon paste. All the data are the average of two reproducible and independent measurements; errors were determined by the standard deviation.

Thus, the above results indicate that the three M-LDHs exhibit promising performances as WOCs in terms of electrochemical parameters. To evaluate their intrinsic activity, though, it is necessary to estimate the electrochemical TOF,[49] which accounts for the actual quantity of noble metal present in the electrode. The results reported in Table 1 reveal that the activity of Ir(III)- and Ru(III)-doped samples is two to three orders of magnitude higher than that of **IrO_2**. The higher TOF of the three M-LDHs, with respect to the benchmark system, is likely due to the noble-metal centers being highly dispersed and easily accessible in the layered structure of these WOCs, while many of the Ir atoms in the bulk of crystalline **IrO_2** likely

serve only structural rather catalytic purposes. These results therefore confirm that 'diluting' Ir/Ru centers in layered inorganic solids of earth abundant elements represents an effective approach to minimize the utilization of noble-metals, while optimizing catalytic performance in WO.[46]

Chronoamperometric and chronopotentiometric studies

Chronoamperometry and chronopotentiometry techniques were used to explore the durability of the electrodes containing the three M-LDHs. In the former case, a constant potential is applied to the electrode, and the current *vs.* time profile is measured; *vice versa*, in the latter technique, the current density is fixed and the potential necessary to maintain it is monitored. Chronoamperometric experiments were performed at 280 mV in 1 M KOH solutions over six hours. The resulting *J vs. t* profiles are reported in Fig. 4 (see also Fig. S7). Interestingly, the current densities measured for the two Ir(III)-LDHs significantly increase over time, going from 0.8 up to 2.6 mA/cm^2 for **Ir-2** and, even more so, from 1.3 to about 10 mA/cm^2 for **Ir-1**. Analogous observations have been previously reported for other heterogeneous WOCs,[79,80] although the magnitude of such increase is unusually high in the present case, especially concerning **Ir-1**. Conversely, current density drops from about 7 to 2.3 mA/cm^2 in the case of **Ru**, while it remains quite low and constant over time for the reference system **IrO_2** (around 0.6 mA/cm^2). These results indicate that the two electrodes with Ir-LDH undergo continuous activation over time, while the profiles measured for **Ru** are indicative of rather poor durability. The latter finding is in line with the typical low stability issues related to Ru-based anodes, which have been often ascribed to excessive oxidation and consequent dissolution of the metal center under catalytic conditions.[81-83]

To further confirm these conclusions, the catalytic performance of the three M-LDHs in WO was retested after the chronoamperometric analysis, to compare the results with those described in the previous section. A comparison of LSV curves obtained before and after chronoamperometry are reported in Fig. S10 in the ESI, while Table 2 summarizes relevant overpotential and current density values relative to those experiments. In line with expectations, the electrochemical activity of the two iridium-based systems appreciably increases after chronoamperometry tests, both in terms of overpotential at 10 mA/cm^2 and current density at 280 mV. In particular, η_{10} drops from 345 to 277 mV in the case of **Ir-1**, and from 458 to 341 mV for **Ir-2**; at the same time, J_{280} increases by a factor of about five for **Ir-1** (2.41 *vs* 11.3 mA/cm^2), and of about two for **Ir-2** (1.5 *vs* 3.38 mA/cm^2). Instead, the performance of **Ru** declines after chronoamperometry, as expected, as η_{10} increases by 81 mV, and J_{280} decreases by 3.5 mA/cm^2.

Chronopotentiometric measurements, performed at a current density of 10 mA/cm^2 in KOH 1 M, allow to draw analogous conclusions to those derived from chronoamperometry. The overpotential *vs.* time plots in Fig. 5 show that, also in this case, **Ir-1** appears to undergo activation over time, as the

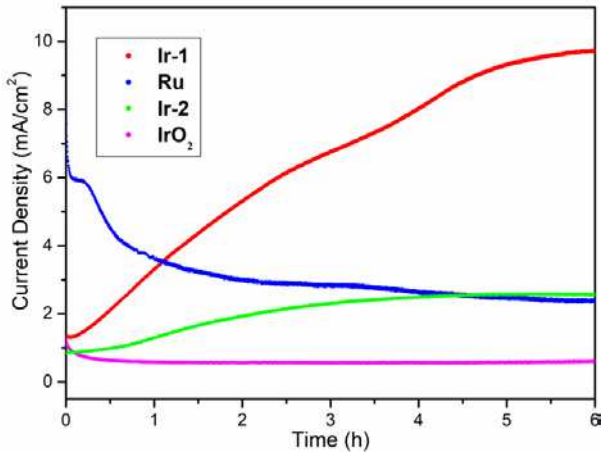

Fig. 4 Current density *vs.* time profiles obtained by chronoamperometry at an overpotential of 280 mV in 1 M KOH.

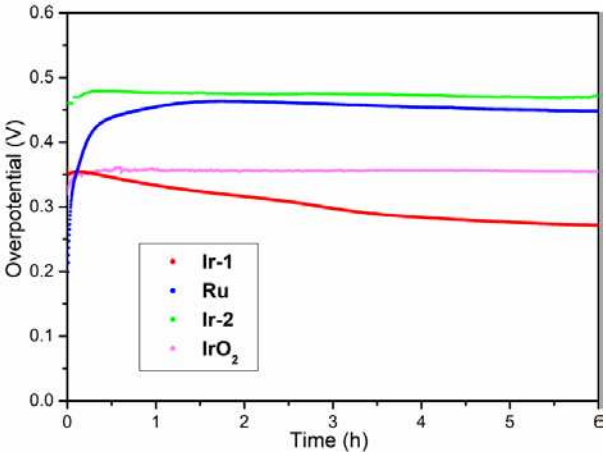

Fig. 5 Overpotential *vs.* time profiles obtained by chronopotentiometry at a current density of 10 mA/Cm^2 in KOH 1 M.

overpotential necessary to keep a current density of 10 mA/cm^2 decreases from 358 to a remarkably value of 270 mV. On the other hand, the overpotential of the other iridium catalyst **Ir-2** remains almost constant over the six hours experiment time, as does that of the benchmark system **IrO_2**,[84] signifying the good durability of these systems. A notable decrease of electrochemical performance is instead observed for **Ru**, as previously highlighted by chronoamperometry, since its overpotential rapidly raises from 200 to 458 mV after only 27 min of chronopotentiometric treatment. Accordingly, catalytic tests performed after chronopotentiometric measurements (Fig. S11 and Table 2) show the expected increase of η_{10} and drop of J_{280} for **Ru** with respect to the first run. Conversely, a marked improvement of catalytic performance is found for **Ir-1** and a milder one for **Ir-2**, both in terms of overpotential and current density. The difference between these two Ir-based systems is likely to be ascribed to the different divalent cations used in the bulk LDH structure (Zn^{2+} *vs.* Mg^{2+}), suggesting that the performances of the active site can be modulated by the proper selection of the low cost and redox-inert matrix metal. This recalls what is occurring in

Table 2 Comparison of electrochemical data obtained by LSV before and after chronoamperometry/chronopotentiometry analysis.[a]

Entry	Catalyst	1st run		After chronoamperometry[b]		After chronopotentiometry[c]	
		J_{280} (mA/cm²)	η_{10} (mV)	J_{280} (mA/cm²)	η_{10} (mV)	J_{280} (mA/cm²)	η_{10} (mV)
1	**Ir-1**	2.4	345	11.2	277	14.4	262
2	**Ru**	11.3	245	7.85	326	9.8	289
3	**Ir-2**	1.5	458	3.38	341	1.83	380

[a] 25°C, 1 M KOH, scan rate 1 mV/s; [b] at 280 mV for 6 h, see also Fig. S10; [c] at 10 mA/cm² for 6 h, see also Fig. S11. J_{280} = current density at 280 mV; η_{10} = overpotential at 10 mA/cm².

the extraordinary WOC developed by Nature, that is the cuboidal Oxygen Evolving Complex, where a redox-inhert calcium ion has a key role in determining the activity of the manganese active sites.[85] Examples of cooperativity between Zn centers and other transition metals have been reported for some oxidation catalysts,[84,87] although further systematic studies would be necessary to draw definitive conclusions on the relationship between composition and catalytic properties of M-LDHs.

Post-catalytic structural characterization

The four LDHs used here were recovered after catalytic tests and characterized in order to evaluate any possible structural changes occurring under WO reaction conditions. Fig. 6 shows a comparison of PXRD patterns obtained before (black) and after (red) electrocatalytic tests, while post-catalysis SEM images are reported in Fig. S6. PXRD patterns maintain the same reflection peaks before and after catalysis. Additional reflections, highlighted with blue asterisks in Fig. 6, are ascribed to the graphitic carbon of electrode materials and remain unvaried before and after catalytic runs. These observations indicate that the structure and crystallinity of the four LDHs appear to be retained after catalytic experiments. The aforementioned activation of **Ir-1** and **Ir-2**, and deactivation of **Ru** over time should therefore be linked to only local, minor structural modifications. Small rearrangements, like clustering of the M-atoms,[88,89] are indeed known to have potentially large effects on catalytic properties, and advanced spectroscopic studies on M-LDHs are currently ongoing in our laboratory to verify this hypothesis. SEM images confirm that no relevant changes in the morphology occurred (Fig. S6).
Furthermore, the supernatant solutions, recovered after electrocatalysis, were analysed by ICP-OES. No appreciable amounts of noble-metals are detected in the liquid phases, indicating that no leaching in solution occurs, in line with previous reports.[46]

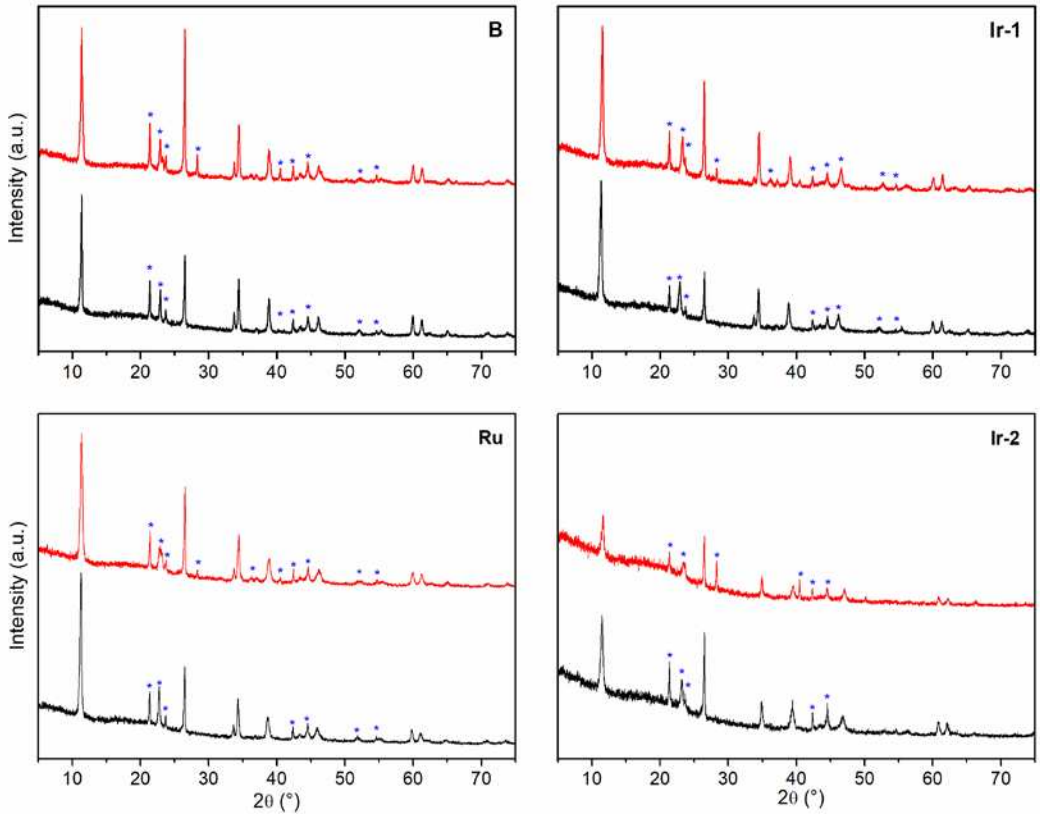

Fig. 6 Comparison between PXRD patterns of the electrodes with undoped LDH (**B**) and the three doped M-LDHs (**Ir-1**, **Ru** and **Ir-2**) before (black) and after (red) electrocatalysis. Blue asterisks indicate the peaks related to carbon black electrode.

Further considerations on the catalytic performance

Based on the results described in the previous sections, it might be concluded that, among the doped LDHs studied here, **Ir-1** is the one exhibiting the overall most satisfying catalytic performance. Indeed, its electrochemical properties are found to be quite good already in the first catalytic run (Table 1), and appreciably improve upon galvanostatic/potentiostatic treatment (Table 2). Eventually, rather low J_{280} of 262-277 mV and very good η_{10} of 11-14 mA/cm^2 are measured, corresponding to TOF higher than 6.8 10^{-3} s^{-1}.

Thus, it is interesting to compare these parameters with those reported for other established WOCs based on LDH. The available literature on these systems is very vast and it has been recently summarized in some excellent reviews.[49,56,60] To name but a few (see also Table S3 for a comparison of η_{10} among representative LDH-based WOCs), successful doping of NiFe LDHs has been accomplished with Cr,[90] Ce,[91] Mn,[92] Ti,[72,93] La[72,93] and noble metals like Ru[89] and Au;[88] in the latter case, single atom Au electrodeposition resulted in η_{10} of only 237 mV and J_{280} above 120 mA/cm^2.[88] Often, the key for enhanced performance appears to lay in the the tuning of structural and morphological properties of the LDH, as reported, for example, for NiFe LDH nanosheets,[72,94] porous NiCoFe layered triple hydroxides (LTH),[94] NiFe hollow microspheres,[95] and exfoliated CoMn LDH nanoplates,[96] all of them exhibiting η_{10} well below 300 mV. Another noteworthy example is the NiFe LDH immobilized on graphene oxide with typical η_{10} around 250 mV.[97,98] It appears therefore that the performance of M-LDHs is still lower than that of leading catalysts of the same class. Nevertheless, considering that the synthesis of M-LDH is very simple, especially compared to some of the aforementioned examples, and that it offers broad possibilities of easy structural tuning, these systems should be definitely amenable to further significant development and performance optimization.

Summary and Conclusions

Three LDHs, doped with very low amounts of Ir(III) and Ru(III) centers (< 2 mol %), have been synthesized and tested as heterogeneous catalysts for electrochemical WO under comparable reaction conditions. When immobilized in carbon paste electrodes, all of them exhibit very good performances, which exceed those of the benchmark system **IrO_2**.

Ru exhibits the best initial performance in terms of necessary overpotential to catalyse WO with only 245 mV at 10 mA/cm^2, although chronoamperometric and chronopotentiometric tests reveal that this system rapidly deactivates over time. Interestingly, its iridium-based analogue **Ir-1** initially exhibits slightly lower performances than **Ru**, especially with respect to current density at 280 mV (2.41 *vs.* 11.3 mA/cm^2, respectively), but it undergoes a considerable activation over time. Indeed, after six hours galvanostatic/potentiostatic treatment, **Ir-1** catalyses OER with good current densities (around 11-14 mA/cm^2) and rather low overpotentials at 10 mA/cm^2 (262-277 mV), which are comparable to those previously mentioned for **Ru**. Furthermore, **Ir-2** exhibits a satisfying durability, although its performance remains lower than that of **Ir-1**. Post-catalytic characterizations reveal that the crystalline structure of these three M-LDHs is preserved, and no significant leaching of iridium or ruthenium in the reaction solutions is detected, signifying a quite good stability of these systems.

The results confirm that doping low-cost layered materials like LDHs with noble metal atoms represents a promising approach to develop effective heterogeneous WOCs, while minimizing the utilization of such precious elements.[46] Overall, the performance of these systems still lower than that of the state-of-art heterogeneous systems of the same type. Nevertheless, the extremely easy and versatile synthesis of M-LDHs, as well as the good activity and electrochemical properties highlighted in this promising but still exploratory study, foster additional investigations aiming at further improve catalytic performance. Reducing the microscale dimensions of these materials to improve the surface-to-bulk ratio and, consequently, the accessibility of the Ir/Ru centers is certainly a possible success strategy, which is being currently explored in our laboratory.

Experimental Section

Materials and Methods

$AlCl_3{\cdot}6H_2O$, $RuCl_3$, $MgCl_2$, fuming HNO_3, synthetic graphite, paraffin wax and KOH were purchased form Sigma-Aldrich, while $ZnCl_2$, $IrCl_3{\cdot}3.7H_2O$ and urea were purchased from Carlo Erba, Alfa Aesar and PlusOne, respectively. All chemicals were used without any further purification. For synthesis and ICP-OES analysis, Milli Q deionized water was used. For the synthesis, water was further decarbonated by prolonged refluxing. The LDHs were synthesized according to literature procedures;[46,66,67] synthetic and characterization details are reported in the ESI.

Electrochemical measurements

Carbon paste was prepared by mixing synthetic graphite (80 wt %) and paraffin wax (20 %).[99] Paraffin wax was heated at about 70°C in an oil bath; when molten, the proper amount of synthetic graphite was added. The blend was mechanically homogenized by prolonged mixing in a mortar. Electrode materials were prepared by adding carbon paste (40 %) to LDHs (60 %), and carefully stirring the resulting blends in a mortar. Electrode materials were pressed in a tip electrode and polished with paper to obtain a mirror surface.

Electrochemical measurements were carried out in a three-electrode set up: carbon paste modified electrode, Pt wire and Ag/AgCl (3 M KCl) were use as working, counter and reference electrodes, respectively. The electrodes were electrochemically activated by 30 cyclic voltammetry (CV) cycles at a potential in the range from -200 to 900 mV *vs* Ag/AgCl at a scan rate of 100 mV/s in 1 M KOH. Electrochemical measurements were performed in 1 M KOH

electrolyte prepared from KOH pellets using Millipore water (resistivity > 15 MΩ/cm). Electrochemical experiments were performed on a high performance potentiostat (autolab PGSTAT302N potentiostat/galvanostat). All measurements are normalized with respect to the geometric surface area of the electrode (0.0314 cm^2). Measurements are reported without any corrections for the Ohmic drop. Potential *vs* Ag/AgCl is correlated to RHE (Reversible Hydrogen Electrode) by the following equations

$$E_{RHE} = E_{Ag/AgCl} + E^0_{Ag/AgCl} + 0.0591 \times pH$$

where $E_{Ag/AgCl}$ is the potential related to Ag/AgCl 3 M reference electrode and $E^0_{Ag/AgCl}$ the standard potential of the electrode. The latter value corresponds to 209 mV *vs*. RHE. As the measured pH was equal to 14, it results:

$$E_{RHE} = E_{Ag/AgCl} + 1036\ mV$$

The overpotential η for the OER was calculated by the following equation:

$$\eta = E_{RHE} - 1230\ mV = E_{Ag/AgCl} - 194\ mV$$

Electrochemical measurements were performed under constant stirring to avoid the formation of oxygen bubbles. Linear sweep voltammetry (LSV) curves were collected at a scan rate of 1 mV/s. Chronoamperometry and chronopotentiometry were carried out at a constant overpotential/current density of 280 mV and 10 mA/cm^2, respectively, in KOH 1M.

Conflicts of interest

There are no conflicts to declare.

Acknowledgements

This work has been financially supported by PRIN 2015 (20154X9ATP_004), University of Perugia and MIUR (AMIS and DELPHI, "Dipartimenti di Eccellenza - 2018-2022" programs), the University of Zurich, the UZH research priority program *Solar Light to Chemical Energy Conversion* (URPP LightChEC) and the Swiss National Science Foundation (Sinergia Grant No. CRSII2_160801/1). F. Z. thanks INSTM and CIRCC for a post-doctoral grant.

Notes and references

1 J. H. Alstrum-Acevedo, M. K. Brennaman and T. J. Meyer, *Inorg. Chem.*, 2005, **44**, 6802–6827.
2 N. S. Lewis and D. G. Nocera, *Proc. Natl. Acad. Sci.*, 2006, **103**, 15729 – 15735.
3 V. Balzani, A. Credi and M. Venturi, *ChemSusChem*, 2008, **1**, 26–58.
4 D. Gust, T. A. Moore and A. L. Moore, *Acc. Chem. Res.*, 2009, **42**, 1890–1898.
5 N. D. McDaniel and S. Bernhard, *Dalton Trans.*, 2010, **39**, 10021–10030.
6 S. Berardi, S. Drouet, L. Francàs, C. Gimbert-Suriñach, M. Guttentag, C. Richmond, T. Stoll and A. Llobet, *Chem. Soc. Rev.*, 2014, **43**, 7501–7519.
7 K. C. Mavrokefalos and R. G. Patzke, *Inorganics* , 2019, **7**, 29.
8 L. Duan, F. Bozoglian, S. Mandal, B. Stewart, T. Privalov, A. Llobet and L. Sun, *Nat. Chem.*, 2012, **4**, 418–423.
9 A. Llobet, *Molecular Water Oxidation Catalysis: A Key Topic for New Sustainable Energy Conversion Schemes*, Wiley-Interscience, New York, 2014.
10 J. Creus, R. Matheu, I. Peñafiel, D. Moonshiram, P. Blondeau, J. Benet-Buchholz, J. García-Antón, X. Sala, C. Godard and A. Llobet, *Angew. Chem. Int. Ed.*, 2016, **55**, 15382–15386.
11 D. L. Gerlach, S. Bhagan, A. A. Cruce, D. B. Burks, I. Nieto, H. T. Truong, S. P. Kelley, C. J. Herbst-Gervasoni, K. L. Jernigan, M. K. Bowman, S. Pan, M. Zeller and E. T. Papish, *Inorg. Chem.*, 2014, **53**, 12689–12698.
12 Z. Codolà, L. Gómez, S. T. Kleespies, L. Que Jr, M. Costas and J. Lloret-Fillol, *Nat. Commun.*, 2015, **6**, 5865.
13 J. Li, R. Güttinger, R. Moré, F. Song, W. Wan and G. R. Patzke, *Chem. Soc. Rev.*, 2017, 46, 6124–6147.
14 M. Okamura, M. Kondo, R. Kuga, Y. Kurashige, T. Yanai, S. Hayami, V. K. K. Praneeth, M. Yoshida, K. Yoneda, S. Kawata and S. Masaoka, *Nature*, 2016, **530**, 465–468.
15 A. Annunziata, R. Esposito, G. Gatto, M. E. Cucciolito, A. Tuzi, A. Macchioni and F. Ruffo, *Eur. J. Inorg. Chem.*, 2018, **2018**, 3304–3311.
16 F. Song, R. Moré, M. Schilling, G. Smolentsev, N. Azzaroli, T. Fox, S. Luber and G. R. Patzke, *J. Am. Chem. Soc.*, 2017, **139**, 14198–14208.
17 I. Corbucci, F. Zaccaria, R. Heath, G. Gatto, C. Zuccaccia, M. Albrecht and A. Macchioni, *ChemCatChem*, In Press, DOI:10.1002/cctc.201901092.
18 Z. Chen, J. J. Concepcion, X. Hu, W. Yang, P. G. Hoertz and T. J. Meyer, *Proc. Natl. Acad. Sci. U. S. A.*, 2010, **107**, 7225–7229.
19 A. Savini, A. Bucci, M. Nocchetti, R. Vivani, H. Idriss and A. Macchioni, *ACS Catal.*, 2015, **5**, 264–271.
20 G. Pastori, K. Wahab, A. Bucci, G. Bellachioma, C. Zuccaccia, J. Llorca, H. Idriss and A. Macchioni, *Chem. – Eur. J.*, 2016, **22**, 13459–13463.
21 K. L. Materna, B. Rudshteyn, B. J. Brennan, M. H. Kane, A. J. Bloomfield, D. L. Huang, D. Y. Shopov, V. S. Batista, R. H. Crabtree and G. W. Brudvig, *ACS Catal.*, 2016, **6**, 5371–5377.
22 K. L. Materna, R. H. Crabtree and G. W. Brudvig, *Chem. Soc. Rev.*, 2017, **46**, 6099–6110.
23 S. W. Sheehan, J. M. Thomsen, U. Hintermair, R. H. Crabtree, G. W. Brudvig and C. A. Schmuttenmaer, *Nat. Commun.*, 2015, **6**, 6469.
24 G. Gatto, A. Macchioni, R. Bondi, F. Marmottini and F. Costantino, *Inorganics*, 2019, **7**, 123.
25 X. Wan, L. Wang, C.-L. Dong, G. Menendez Rodriguez, Y.-C. Huang, A. Macchioni and S. Shen, *ACS Energy Lett.*, 2018, **3**, 1613–1619.
26 D. Ressnig, M. Shalom, J. Patscheider, R. Moré, F. Evangelisti, M. Antonietti and G. R. Patzke, *J. Mater. Chem. A*, 2015, **3**, 5072–5082.
27 C. Wang, J. Wang and W. Lin, *J. Am. Chem. Soc.*, 2012, **134**, 19895–19908.
28 C. C. L. McCrory, S. H. Jung, J. C. Peters and T. F. Jaramillo, *J. Am. Chem. Soc.*, 2013, **135**, 16977–16987.

29 H. Liu, R. Moré, H. Grundmann, C. Cui, R. Erni and G. R. Patzke, *J. Am. Chem. Soc.*, 2016, **138**, 1527–1535.
30 M. W. Kanan and D. G. Nocera, *Science*, 2008, **321**, 1072–1075.
31 S. Cherevko, S. Geiger, O. Kasian, N. Kulyk, J.-P. Grote, A. Savan, B. R. Shrestha, S. Merzlikin, B. Breitbach, A. Ludwig and K. J. J. Mayrhofer, *Catal. Today*, 2016, **262**, 170–180.
32 Y. Lee, J. Suntivich, K. J. May, E. E. Perry and Y. Shao-Horn, *J. Phys. Chem. Lett.*, 2012, **3**, 399–404.
33 X. Liang, L. Shi, Y. Liu, H. Chen, R. Si, W. Yan, Q. Zhang, G.-D. Li, L. Yang, X. Zou, *Angew. Chem. Int. Ed.* 2019, **58**, 7631 –7635
34 R. Matheu, P. Garrido-Barros, M. Gil-Sepulcre, M. Z. Ertem, X. Sala, C. Gimbert-Suriñach and A. Llobet, *Nat. Rev. Chem.*, 2019, **3**, 331–341.
35 A. Macchioni, *Eur. J. Inorg. Chem.*, 2019, **2019**, 7–17.
36 R. Matheu, M. Z. Ertem, J. Benet-Buchholz, E. Coronado, V. S. Batista, X. Sala and A. Llobet, *J. Am. Chem. Soc.*, 2015, **137**, 10786–10795.
37 I. Corbucci, A. Macchioni, M. Albrecht, Iridium Complexes in Water Oxidation Catalysis, in *Iridium(III) in Optoelectronic and Photonics Applications* (Eds.: Zysman-Colman, E.), John Wiley & Sons Ltd: Hoboken, NJ, 2017.
38 B. M. Hunter, H. B. Gray and A. M. Müller, *Chem. Rev.*, 2016, **116**, 14120–14136.
39 M. D. Kärkäs and B. Åkermark, *Dalton Trans.*, 2016, **45**, 14421–14461.
40 C. Casadevall, A. Bucci, M. Costas and J. Lloret-Fillol, *Adv. Organomet. Chem.*, 2019, **74**, 151-196.
41 M. Ledendecker, S. Geiger, K. Hengge, J. Lim, S. Cherevko, A. M. Mingers, D. Göhl, G. V. Fortunato, D. Jalalpoor, F. Schüth, C. Scheu, K. J. J. Mayrhofer, *Nano Res.* 2019, **12**, 2275–2280
42 C. Zuccaccia, G. Bellachioma, S. Bolaño, L. Rocchigiani, A. Savini and A. Macchioni, *Eur. J. Inorg. Chem.*, 2012, **2012**, 1462–1468.
43 C. Zuccaccia, G. Bellachioma, O. Bortolini, A. Bucci, A. Savini and A. Macchioni, *Chem. - Eur. J.*, 2014, **20**, 3446–3456.
44 F. Cavani, F. Trifirò and A. Vaccari, *Catal. Today*, 1991, **11**, 173–301.
45 Q. Wang and D. O'Hare, *Chem. Rev.*, 2012, **112**, 4124–4155.
46 L. Fagiolari, A. Scafuri, F. Costantino, R. Vivani, M. Nocchetti and A. Macchioni, *ChemPlusChem*, 2016, **81**, 1060–1063.
47 G. Alberti and U. Costantino, in *Comprehensive Supramolecular Chemistry, Vol. 7: Solid-State Supramolecular Chemistry*, eds. G. Alberti and T. Bein, Pergamon, Oxford (UK), 1996.
48 S. Nayak, L. Mohapatra and K. Parida, *J. Mater. Chem. A*, 2015, **3**, 18622–18635.
49 Z. Cai, X. Bu, P. Wang, J. C. Ho, J. Yang and X. Wang, *J. Mater. Chem. A*, 2019, **7**, 5069–5089.
50 G. Liu, L. Wang, H. G. Yang, H.-M. Cheng and G. Q. Lu, *J. Mater. Chem.*, 2010, **20**, 831–843.
51 P. Kanhere and Z. Chen, *Molecules*, 2014, **19**, 19995-20022.
52 M.-Q. Zhao, Q. Zhang, J.-Q. Huang and F. Wei, *Adv. Funct. Mater.*, 2012, **22**, 675–694.
53 Y. Zhao, P. Chen, B. Zhang, D. S. Su, S. Zhang, L. Tian, J. Lu, Z. Li, X. Cao, B. Wang, M. Wei, D. G. Evans and X. Duan, *Chem. – Eur. J.*, 2012, **18**, 11949–11958.
54 G. Fan, F. Li, D. G. Evans and X. Duan, *Chem. Soc. Rev.*, 2014, **43**, 7040–7066.
55 A. C. S. Alcântara, P. Aranda, M. Darder and E. Ruiz-Hitzky, *J. Mater. Chem.*, 2010, **20**, 9495–9504.
56 X. Long, Z. Wang, S. Xiao, Y. An and S. Yang, *Mater. Today*, 2016, **19**, 213–226.
57 Y. Zhao, X. Jia, G. I. N. Waterhouse, L.-Z. Wu, C.-H. Tung, D. O'Hare and T. Zhang, *Adv. Energy Mater.*, 2016, **6**, 1501974.
58 L. Zhou, M. Shao, M. Wei and X. Duan, *J. Energy Chem.*, 2017, **26**, 1094–1106.
59 M. Gong, Y. Li, H. Wang, Y. Liang, J. Z. Wu, J. Zhou, J. Wang, T. Regier, F. Wei and H. Dai, *J. Am. Chem. Soc.*, 2013, **135**, 8452–8455.
60 Y. Wang, D. Yan, S. El Hankari, Y. Zou and S. Wang, *Adv. Sci.*, 2018, **5**, 1800064.
61 D. Tang, J. Liu, X. Wu, R. Liu, X. Han, Y. Han, H. Huang, Y. Liu and Z. Kang, *ACS Appl. Mater. Interfaces*, 2014, **6**, 7918–7925.
62 A. Bucci, A. Savini, L. Rocchigiani, C. Zuccaccia, S. Rizzato, A. Albinati, A. Llobet and A. Macchioni, *Organometallics*, 2012, **31**, 8071–8074.
63 G. Menendez Rodriguez, A. Bucci, R. Hutchinson, G. Bellachioma, C. Zuccaccia, S. Giovagnoli, H. Idriss and A. Macchioni, *ACS Energy Lett.*, 2017, **2**, 105–110.
64 G. M. Rodriguez, G. Gatto, C. Zuccaccia and A. Macchioni, *ChemSusChem*, 2017, **10**, 4503–4509.
65 J. Kiwi and M. Grätzel, *Angew. Chem. Int. Ed. Eng.*, 1978, **17**, 860–861.
66 M. Bastianini, D. Costenaro, C. Bisio, L. Marchese, U. Costantino, R. Vivani and M. Nocchetti, *Inorg. Chem.*, 2012, **51**, 2560–2568.
67 U. Costantino, F. Marmottini, M. Nocchetti and R. Vivani, *Eur. J. Inorg. Chem.*, 1998, **1998**, 1439–1446.
68 U. Costantino, M. Casciola, L. Massinelli, M. Nocchetti and R. Vivani, *Solid State Ionics*, 1997, **97**, 203–212.
69 H. M. Rietveld, *J. Appl. Crystallogr.*, 1969, **2**, 65–71.
70 R. D. Shannon, *Acta Crystallogr.*, 1976, **A32**, 751.
71 F. Basile, G. Fornasari, M. Gazzano and A. Vaccari, *Appl. Clay Sci.*, 2000, **16**, 185–200.
72 B. M. Hunter, J. D. Blakemore, M. Deimund, H. B. Gray, J. R. Winkler and A. M. Müller, *J. Am. Chem. Soc.*, 2014, **136**, 13118–13121.
73 B. Hannoyer, M. Ristic, S. Popovic, S. Music, F. Petit, B. Foulon, S. Dalipi, *Mater. Chem. Phys.* 1998, **55**, 215-223.
74 The Ag/AgCl electrode was carefully washed after every catalytic run and the electrolyte solution frequently regenerated to prevent formation of AgOH and/or AgO (see M. Jin, J. Xu, L. Jiang, Y. Xu and H. Chu, *Ionics* 2015, **21**, 2981–2992); no evident signs of electrode deterioration were observed.
75 R. L. LeRoy, *Int. J. Hydrogen Energy*, 1983, **8**, 401-417.
76 10 mA/cm^2 is the current density expected for a 10 % efficiency solar-to-fuel conversion device under one sun illumination; see C. C. L. McCrory, S. Jung, I. M. Ferrer, S. M. Chatman, J. C. Peters and T. F. Jaramillo, *J. Am. Chem. Soc.* 2015, **137**, 4347–4357.
77 F. Song and X. Hu, *Nat. Commun.*, 2014, **5**, 4477.
78 T. Nakagawa, C. A. Beasley and R. W. Murray, *J. Phys. Chem. C*, 2009, **113**, 12958–12961.
79 X. Cao, E. Johnson and M. Nath, *J. Mater. Chem. A*, 2019, **7**, 9877–9889.
80 K. Fan, H. Chen, Y. Ji, H. Huang, P. M. Claesson, Q. Daniel, B. Philippe, H. Rensmo, F. Li, Y. Luo and L. Sun, *Nat. Commun.*, 2016, **7**, 11981.

81 J. Yu, Q. He, G. Yang, W. Zhou, Z. Shao, M. Ni, *ACS Catal.* 2019, **9**, 9973−10011.
82 O. Kasian, S. Geiger, P. Stock, G. Polymeros, B. Breitbach, A. Savan, A. Ludwig, S. Cherevko,K. J. J. Mayrhofer, *J. Electrochem. Soc.* 2016, **163**, F3099-F3104.
83 R. Kotz, R. Stucki, *Electrochim. Acta* 1986, **31**, 1311-1316.
84 J. Suntivich, K. J. May, H. A. Gasteiger, J. B. Goodenough and Y. Shao-Horn, *Science,* 2011, **334**, 1383 – 1385.
85 R. E. Blankenship, *Molecular Mechanisms of Photosynthesis*, Blackwell Science, Oxford, 2002.
86 L. Ni, R. Güttinger, C. A. Triana, B. Spingler, K. K. Baldridge and G. R. Patzke, *Dalton Trans.*, 2019, **48**, 13293–13304.
87 M. K. Karunananda, F. X. Vázquez, E. E. Alp, W. Bi, S. Chattopadhyay, T. Shibata and N. P. Mankad, *Dalton Trans.*, 2014, **43**, 13661–13671.
88 J. Zhang, J. Liu, L. Xi, Y. Yu, N. Chen, S. Sun, W. Wang, K. M. Lange and B. Zhang, *J. Am. Chem. Soc.*, 2018, **140**, 3876–3879.
89 Z. Wang, S.-M. Xu, Y. Xu, L. Tan, X. Wang, Y. Zhao, H. Duan and Y.-F. Song, *Chem. Sci.*, 2019, **10**, 378–384.
90 Y. Yang, L. Dang, M. J. Shearer, H. Sheng, W. Li, J. Chen, P. Xiao, Y. Zhang, R. J. Hamers and S. Jin, *Adv. Energy Mater.*, 2018, **8**, 1703189.
91 H. Xu, B. Wang, C. Shan, P. Xi, W. Liu and Y. Tang, *ACS Appl. Mater. Interfaces*, 2018, **10**, 6336–6345.
92 D. Zhou, Z. Cai, Y. Jia, X. Xiong, Q. Xie, S. Wang, Y. Zhang, W. Liu, H. Duan and X. Sun, *Nanoscale Horizons*, 2018, **3**, 532–537.
93 B. M. Hunter, W. Hieringer, J. R. Winkler, H. B. Gray and A. M. Müller, *Energy Environ. Sci.*, 2016, **9**, 1734–1743.
94 A.-L. Wang, H. Xu and G.-R. Li, *ACS Energy Lett.*, 2016, **1**, 445–453.
95 C. Zhang, M. Shao, L. Zhou, Z. Li, K. Xiao and M. Wei, *ACS Appl. Mater. Interfaces*, 2016, **8**, 33697–33703.
96 F. Song and X. Hu, *J. Am. Chem. Soc.*, 2014, **136**, 16481–16484.
97 X. Yu, M. Zhang, W. Yuan and G. Shi, *J. Mater. Chem. A*, 2015, **3**, 6921–6928.
98 D. H. Youn, Y. Bin Park, J. Y. Kim, G. Magesh, Y. J. Jang and J. S. Lee, *J. Power Sources*, 2015, **294**, 437–443.
99 R. N. Adams, *Anal. Chem.*, 1958, **30**, 1576.